Journal of Power Sources 183 (2008) 701–707

Contents lists available at ScienceDirect

Journal of Power Sources

journal homepage: www.elsevier.com/locate/jpowsour

Synthesis and high photocatalytic hydrogen production of $SrTiO_3$ nanoparticles from water splitting under UV irradiation

Yang Liu[a,c], Lei Xie[a], Yan Li[a], Rong Yang[a], Jianglan Qu[a], Yaoqi Li[a], Xingguo Li[a,b,*]

[a] Beijing National Laboratory for Molecular Sciences (BNLMS), The State Key Laboratory of Rare Earth Materials Chemistry and Applications, College of Chemistry and Molecular Engineering, Peking University, Beijing 100871, China
[b] College of Engineering, Peking University, Beijing 100871, China
[c] Beijing Key Laboratory of Bioactive Substances and Functional Foods, College of Arts and Science, Beijing Union University, Beijing 100083, China

ARTICLE INFO

Article history:
Received 5 May 2008
Accepted 20 May 2008
Available online 28 May 2008

Keywords:
Photocatalyst
Water splitting
Hydrogen
Polymerized complex method

ABSTRACT

Cubic $SrTiO_3$ powders were synthesized by three methods: the polymerized complex (PC) method, the solid state reaction, and the milling assistant method. The samples obtained were characterized by X-ray diffraction (XRD), UV–vis spectroscopy (UV–vis), scanning electron microscopy (SEM), and transmission electron microscopy (TEM). The mean diameters of the as-synthesized $SrTiO_3$ particles were 30 nm by the polymerized complex method, 140 nm by the solid state reaction, and 30 nm by the milling assistant method. The photocatalytic activity of hydrogen evolution from water splitting over $SrTiO_3$ powders by the polymerized complex method is higher than that by the solid state reaction and the milling assistant method. Particle size, uniformity of components, and particle aggregation extent affect the photocatalytic activity of $SrTiO_3$ for hydrogen evolution. The best rate of photocatalytic hydrogen evolution over $SrTiO_3$ by the polymerized complex method under UV illumination is as high as 3.2 mmol h^{-1} g^{-1}.

1. Introduction

Recently, great interest has focused on photocatalytic water splitting, because H_2 with its high-energy capacity and environmental friendliness could be obtained from clean and renewable water and solar energy. In 1972, Fujishima and Honda [1] produced hydrogen through photochemical catalysis using TiO_2 under UV light. Since then, photocatalytic hydrogen production over semiconductors has attracted more interest in the field of clean energy research. When light irradiates semiconductors, electrons and holes are produced. Photogenerated electrons with reducibility can reduce H_2O into hydrogen. Semiconductors must meet three requirements if they are to split water to generate hydrogen: (1) conduction bands must locate above the potential of water reduction (E_{0H+/H_2}); (2) the band gap of semiconductors must be more than the potential of water splitting; and (3) semiconductor photocatalysts must be stable and durable. [2] Many semiconductors such as transition metal oxides TiO_2 [3,4], $SrTiO_3$ [5], $K_2La_2Ti_3O_{10}$ [6], Ta_2O_5 [7], and Nb_2O_5 [8] are used as photocatalysts to split water for hydrogen generation. Among the vast majority of metal oxide photocatalysts, perovskite-type oxides are prominent for their diversity of properties. The ideal perovskite-type cubic structure of ABO_3 provides the flexibility to vary the composition of the A and B sites to form substituted perovskites. The A cation is 12-fold coordinated and the B cation is 6-fold coordinated with the oxygen anions. The corner-sharing BO_6 octahedra form the skeleton of the structure, in which the center position is occupied by the A cation. Strontium titanate ($SrTiO_3$) is a dielectric material, and is used as a photocatalyst to degrade organic pollutants or split water to produce hydrogen and oxygen [9–11]. Perovskite-type $SrTiO_3$ provides a higher potential than TiO_2 and facilitates the formation of hydrogen and oxygen [12].

$SrTiO_3$ as a photocatalyst could be used to produce hydrogen under UV light. $SrTiO_3$ is conveniently prepared by solid state reaction. The mixture of $SrCO_3$ and TiO_2 is calcined at above 1000 °C for 10 h. The size of as-synthesized $SrTiO_3$ particles is about 1–2 μm. In general, NiO is deposited on the surface of $SrTiO_3$ particles, and NiO-$SrTiO_3$ is used to generate hydrogen by splitting water under UV light [13–17]. The alkoxide method could be used to synthesize $SrTiO_3$, but the size of $SrTiO_3$ is about 0.1–0.2 μm, and the phases of $SrTiO_3$ are not single cubic [18].

The polymerized complex method has been used to synthesize titanate, tantalite, and niobate, such as M-doped $La_2Ti_2O_7$ (M = Cr,

* Corresponding author at: Beijing National Laboratory for Molecular Sciences (BNLMS), The State Key Laboratory of Rare Earth Materials Chemistry and Applications, College of Chemistry and Molecular Engineering, Peking University, Beijing 100871, China. Tel.: +86 10 6276 5930; fax: +86 10 6276 5930.
E-mail address: xgli@pku.edu.cn (X. Li).

0378-7753/$ – see front matter © 2008 Elsevier B.V. All rights reserved.
doi:10.1016/j.jpowsour.2008.05.057

Fe) [19], $Sr_3Ti_2O_7$ [20], R_3MO_7, and $R_2Ti_2O_7$ (R = Y, Gd, La; M = Nb, Ta) [21]. However, it is not easy to synthesize pure cubic $SrTiO_3$ through the PC method.

In this study, we prepared $SrTiO_3$ via the PC, solid state reaction, and milling assistant methods. In the solid state reaction, we used P25 (Degussa, 25 nm) as one raw material, while in the classic solid state reaction, TiO_2 with large size (1 μm) was used. In our work, the milling assistant method is first presented to synthesize nano-sized $SrTiO_3$. We studied the photocatalytic activities of hydrogen evolution over $SrTiO_3$ through three methods under UV light.

2. Experimental

2.1. Photocatalyst preparation

In the PC method, 3.4 g $Ti(OC_4H_9)_4$ was dissolved in glycol. The mixture was heated at 50 °C for 30 min. 0.2 mol acetic acid was added into the above mixture solution. The solution was heated under stirring at 120 °C for about 4 h until it became transparent. 2.12 g $Sr(NO_3)_2$ was added and dissolved immediately. The transparent solution was heated at 120 °C for about 10 h until its color became deep brown. The deep brown resin was cooled to room temperature. The resin was heated in a stove at 300 °C for 3 h. The as produced precursor of $SrTiO_3$ was calcined at 500, 600, 700, 800, and 1000 °C for 5 h. The samples were therefore named PC500, PC600, PC700, PC800, and PC1000.

In the solid state reactions, 0.18 g TiO_2 (Degussa P25) and 0.32 g $SrCO_3$ were mixed through an agate mortar, then calcined at 800 and 1000 °C for several hours. In order to determine the effects of preliminary treatment time on the photocatalytic activity of hydrogen evolution by splitting water, we calcined the reactants at 800 °C for 3 h (named as S800/3) following at 1000 °C for 3 h, and the product was named as S800/3/1000/3. The reactants were calcined at 800 °C for 5 h following at 1000 °C for 3 h, and the product was named S800/5/1000/3. The reactants were calcined at 800 °C for 5 h, and the product was named S800/5.

In milling assistant method, the stoichiometric proportions of P25 and $SrCO_3$ were mechanically milled for 12 h at 300 rpm using a planetary ball milling apparatus (Pulverisette 5). The sample mass was 2.5 g and the ball-to-sample weight ratio was about 37:1 in each milling process. The as-produced precursor was named Q/12. Q/12 was calcined at 800 °C for 2 h. The resulting product was named Q800/2.

To make photocatalytic hydrogen evolve easily, the cocatalyst Pt (0.32 wt%, relative to the amount of photocatalyst) was loaded on the surface of as-prepared $SrTiO_3$ samples by photodeposition methods. 0.08 g $SrTiO_3$ powder dispersed in 20 mL ethanol solution. 0.038 M H_2PtCl_6 was added. Argon was used to purge out air in the solution. A 500 W high-pressure mercury lamp was used to irradiate the solution under stirring for 1 h. The photocatalyst powder deposited with Pt was separated using a centrifuger, washed with ethanol, and dried at 70 °C overnight.

2.2. Photocatalyst characterization

The crystal structure of the $SrTiO_3$ samples was determined by X-ray powder diffraction on an X-ray powder diffractometer (Rigaku D/MAX 200) with a Cu target Kα irradiation (λ = 1.5401 Å) at 40 KV and 100 mA. The scan rate was 4° min^{-1}. The optical properties of $SrTiO_3$ were analyzed by a UV–vis diffuse reflectance spectrometer (Shimadzu, UV2401PC). Scanning electron microscopy (SEM) (Hitachi S4800, 10 kV) and transmission electron microscopy (TEM) (JEOL JEM-200 CX) were used to observe the morphology of samples. Differential scanning calorimetry (DSC) associated with a thermogravimetric analyzer (TGA) (Q600 SDT) was employed to determine the calcination temperature (Al_2O_3 crucible, 10 °C min^{-1}, in air). Inductively coupled plasma spectrometry (ICP-AES) analysis was carried out to determine the metal ions in the samples (Profile-ICP-AES, Leeman Labs. Inc., USA).

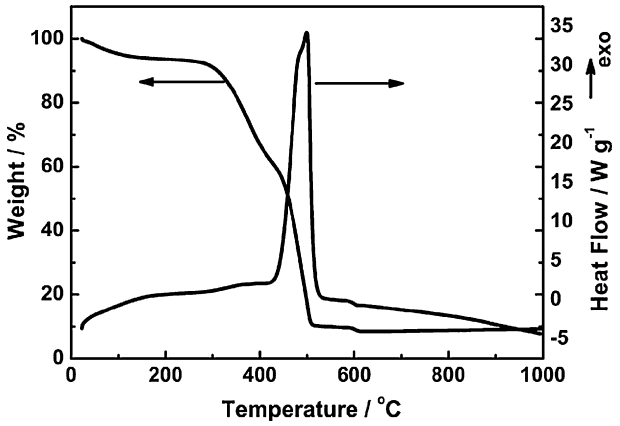

Fig. 1. TGA and DSC data of $SrTiO_3$ synthesized through the PC method.

2.3. Photocatalytic reaction

The photocatalytic hydrogen generation was carried out in a Pyrex glass container with a volume of 320 mL. A 500 W high-pressure mercury lamp (center wavelength 365 nm) equipped with cooling water was used as an irradiation source, which was placed at a fixed distance from the photocatalytic reactor. The intensity of irradiation was 5.5 mW cm^{-2}. The photocatalytic reaction of water splitting was performed in a 60 mL solution (35 mL distilled water and 25 mL methanol as sacrificial agent). 0.06 g photocatalyst was added into the solution. Before the mercury lamp was turned on, the suspension was thoroughly degassed through introducing argon into the system to purge out dissolved oxygen for 30 min. After the lamp was turned on, the solution was stirred. To maintain the reaction temperature constant at 25 °C, the photocatalytic reaction system was equipped with an electric fan. The evolved hydrogen was measured with gas chromatography (GC, SP3420, MS-5A, TCD, Ar carrier).

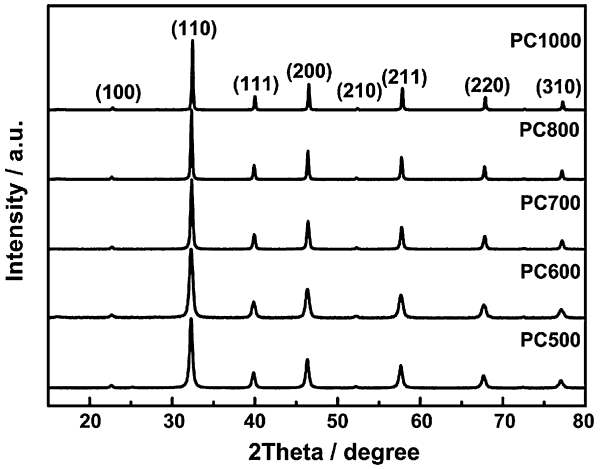

Fig. 2. XRD patterns of $SrTiO_3$ samples synthesized by PC method (PC500, PC600, PC700, PC800, and PC1000).

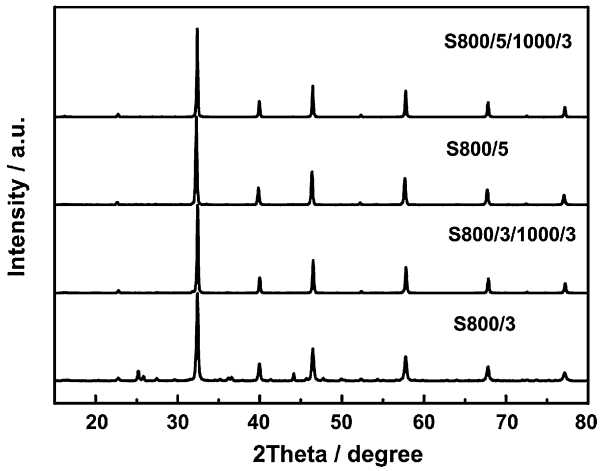

Fig. 3. XRD patterns of $SrTiO_3$ samples synthesized by solid state method (S800/3, S800/3/1000/3, S800/5, S800/5/1000/3).

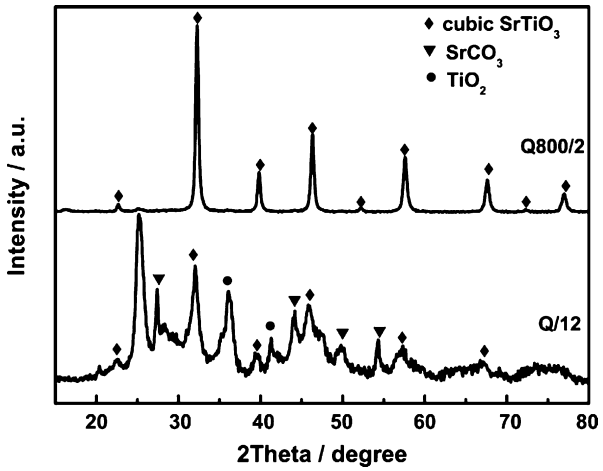

Fig. 4. XRD patterns of $SrTiO_3$ synthesized by ball milling assistant methods (Q/12 and Q800/2).

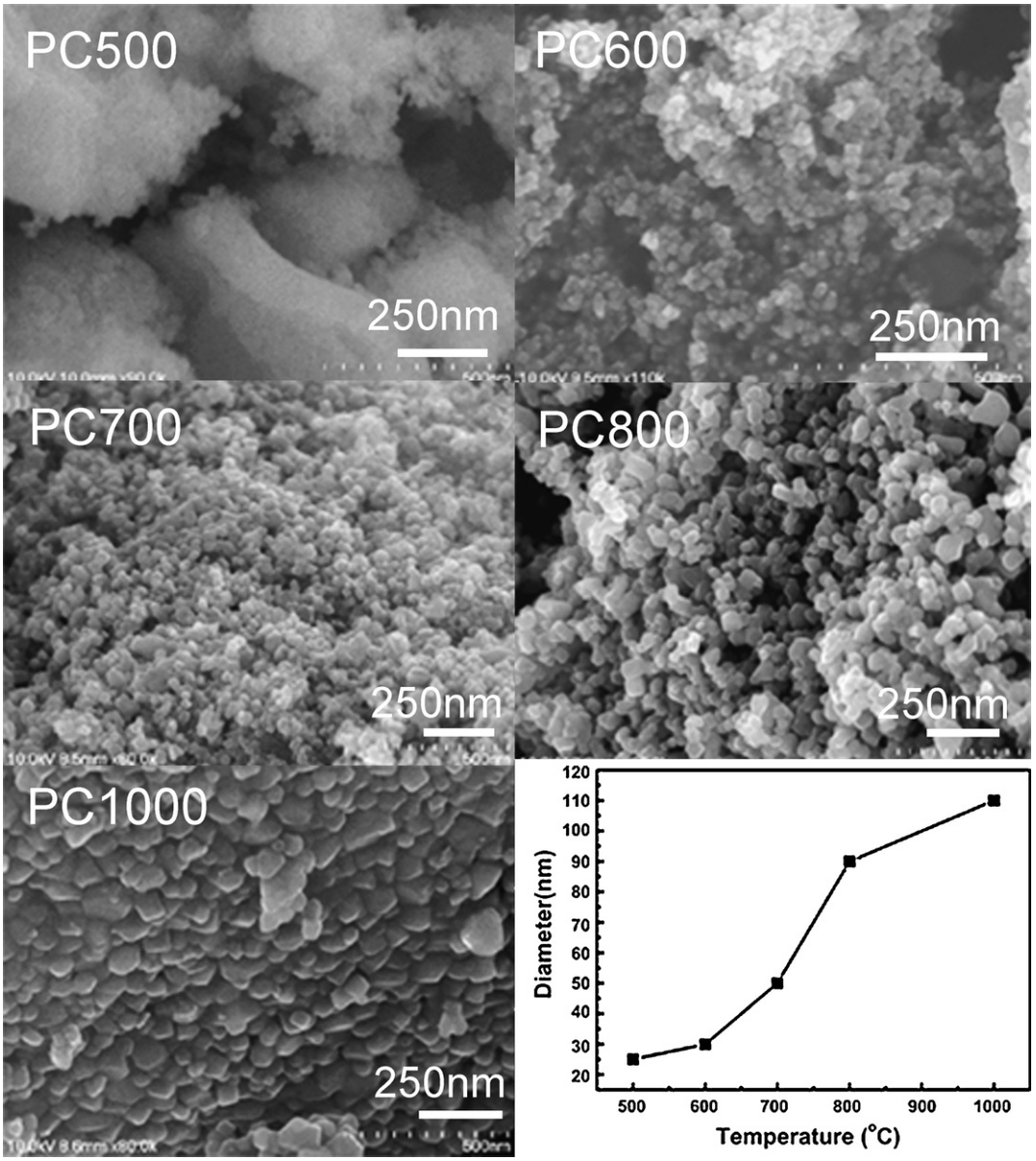

Fig. 5. SEM of $SrTiO_3$ synthesized by PC method (PC500, PC600, PC700, PC800, and PC1000) and the change of average diameter of $SrTiO_3$ with calcination temperature.

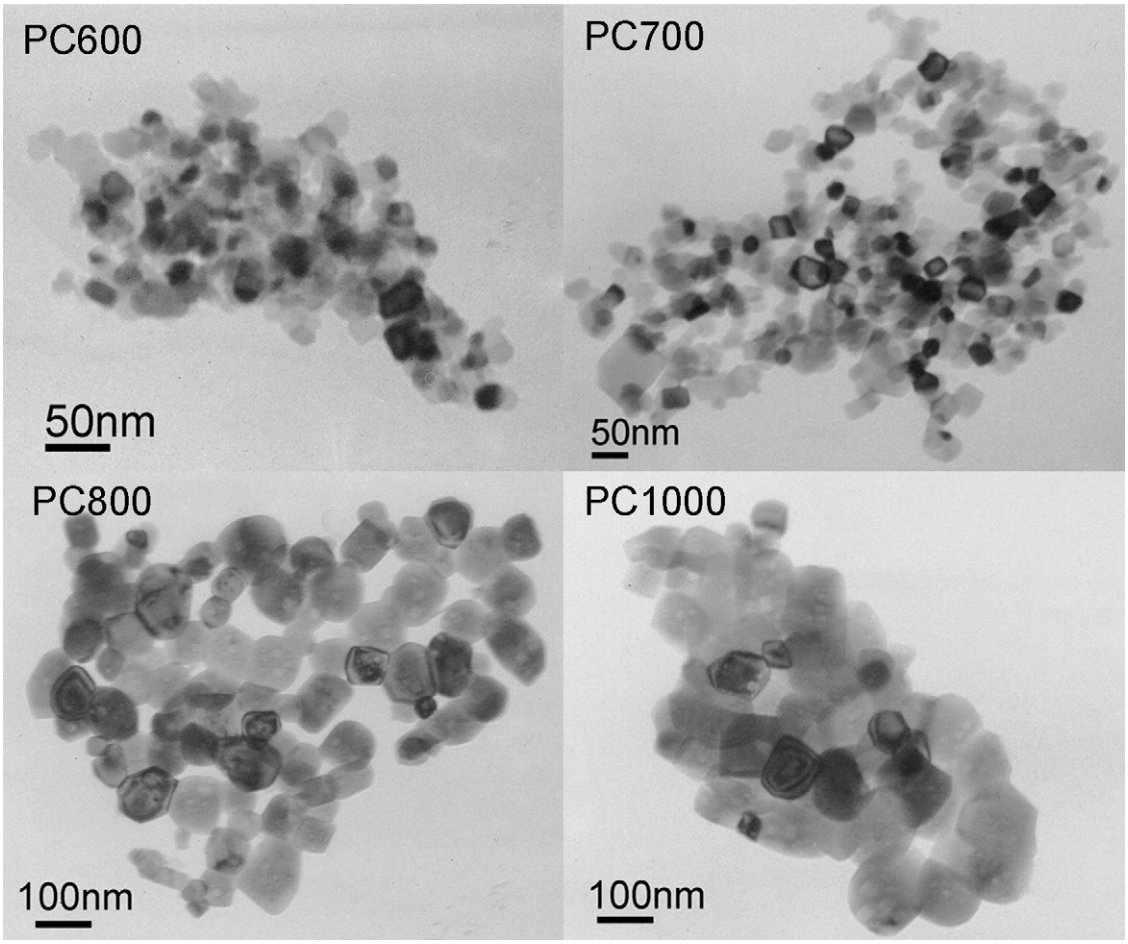

Fig. 6. TEM of $SrTiO_3$ synthesized by PC method (PC600, PC700, PC800, and PC1000).

3. Results and discussions

3.1. TGA/DSC analysis, XRD, SEM, and TEM

The TGA/DSC analysis of the $SrTiO_3$ precursor through the PC method (Fig. 1) shows a major weight loss of about 83% in the range of 25–500 °C, which is due to the elimination of a majority of organic compounds. 8% of weight loss occurs in the range of 500–600 °C because of the elimination of remnant carbons in $SrTiO_3$ samples. No weight loss occurs above 600 °C. In order to remove organic compounds completely, the lowest calcination temperature must be above 600 °C.

Fig. 2 shows XRD patterns of $SrTiO_3$ synthesized by the PC method. PC500, PC600, PC700, PC800, and PC1000 have a pure cubic structure (JCPDS74-1296). The strongest diffraction peak, located at 32.46°, belongs to the (1 1 0) plane.

Fig. 3 shows the XRD results of $SrTiO_3$ synthesized by the solid state method. S800/3 has no pure cubic structure. In the solid state reaction, 3 h is not enough to obtain the pure cubic structure for $SrTiO_3$ S800/5, S800/3/1000/3, and S800/5/1000/3 samples.

Fig. 4 shows the XRD patterns of Q/12 and Q800/2. Q/12 is not pure $SrTiO_3$. The pure cubic structure could not be obtained when the mixture of P25 and $SrCO_3$ was ball milled for 12 h. If Q/12 was followed by calcination at 800 °C for 2 h, pure cubic Q800/2 was obtained.

The morphology of $SrTiO_3$ synthesized through PC method is shown in Figs. 5 and 6. The sizes of $SrTiO_3$ particles are uniform through the PC method. PC600, PC700, PC800, and PC1000 have average sizes of 30, 40, 90, and 110 nm, respectively. PC500 has the small size of 25 nm. However, impurity carbons exist in PC500. The PC method could provide small size $SrTiO_3$ particles, such as PC600 with the size of 30 nm. In the PC method, the $SrTiO_3$ precursor is surrounded by organic compounds, which prevents the growth of $SrTiO_3$ nucleus. The $SrTiO_3$ particles evidently become bigger with increasing calcination temperature (this result is shown in Fig. 5). The sizes of $SrTiO_3$ increase from 25 to 110 nm with increasing the calcination temperature from 500 to 1000 °C. The growth rate of crystal particles is accelerated at high calcination temperature. In addition, the edges of cubic $SrTiO_3$ particles PC800 and PC1000 become blunt. Many circles appear in PC1000 samples (shown in Fig. 6).

The morphology of $SrTiO_3$ through the solid state and milling assistant methods is shown in Fig. 7. S800/5, S800/3/1000/3, and S800/5/1000/3 have similar particle sizes. The average diameter is about 140–150 nm. In solid state reactions, most heating energy was consumed for transportation and rearrangement of Ti, O, and Sr atoms until cubic $SrTiO_3$ nuclei form. Not enough energy was provided for the growth of $SrTiO_3$ nuclei. S800/5, S800/3/1000/3, and S800/5/1000/3 have smaller sizes than $SrTiO_3$ through the classic solid state method because P25 with small size is used, which shortens the transportation distance. S800/5/1000/3 has been sintered together in some extent at an additional 1000 °C for 3 h.

In Fig. 7, Q800/2 has a small size, about 30 nm. However, many Q800/2 nanoparticles aggregated together. When ball-milled Q12 was calcined at 800 °C, the as-produced Q800/2 inclined to

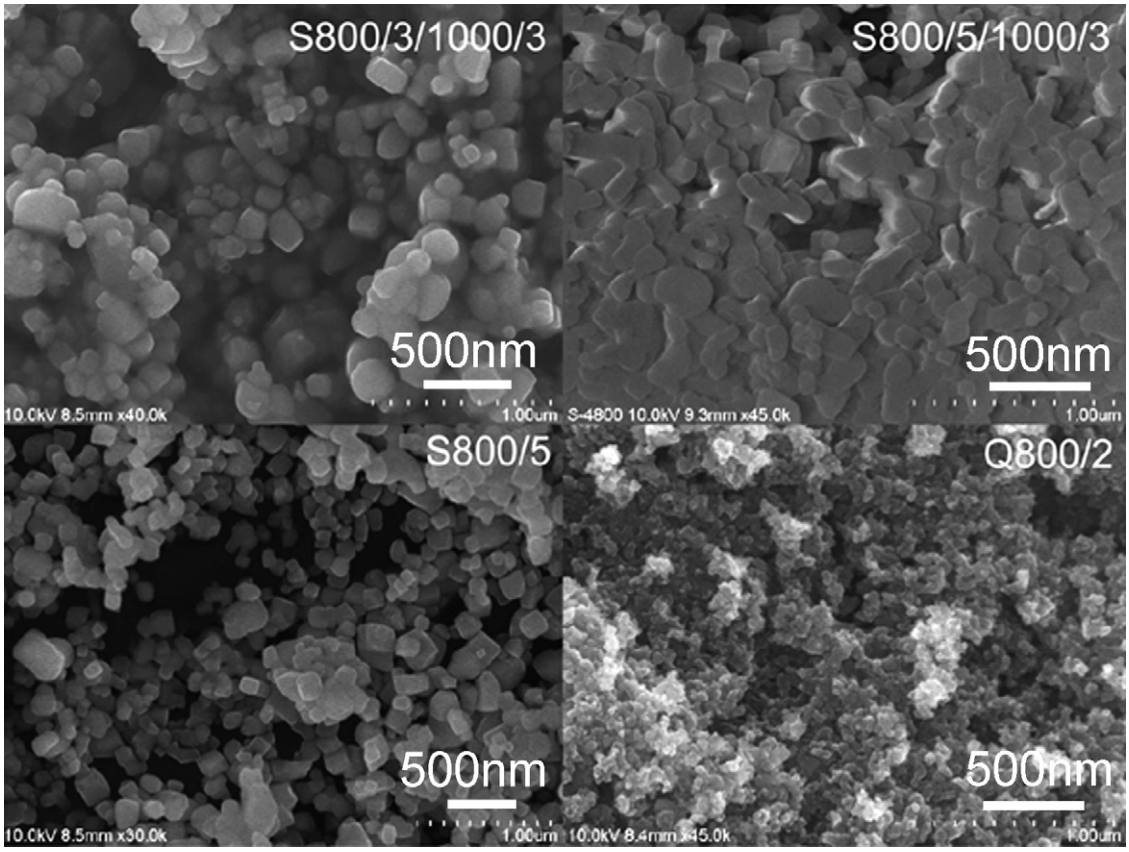

Fig. 7. SEM of $SrTiO_3$ synthesized by solid state method (S800/3/1000/3, S800/5/1000/3, and S800/5) and milling assistant method (Q800/2).

aggregate, and the surface energy of Q800/2 decreased. More average diameter results are shown in Table 1.

3.2. UV–vis diffuse reflectance spectra of samples

UV–vis diffuse reflectance spectra of $SrTiO_3$ synthesized through the PC, solid state, and milling assistant methods are shown in Figs. 8 and 9. According to the plot of square root of $h\nu(A)$ versus $h\nu$ (eV), the band gap of the semiconductor can be obtained. PC500, PC600, PC700, PC800, PC1000, S800/5, S800/3/1000/3, and S800/5/1000/3 can adsorb UV light at wavelengths less than 390 nm (shown in Figs. 8a and 9a), and the band gap is about 3.1 eV (shown in Figs. 8b and 9b). Q800/2 can adsorb visible light with a wavelength of 650 nm and the band gap is about 2.0 eV (shown in Fig. 9a and b). Iron ions were detected through ICP-AES analysis. 0.3 wt% iron ions as impurities have been doped into the lattice of $SrTiO_3$ in the ball milling process. Fe 3d orbits locate above O 2p orbits. Fe 3d has more negative potential than O 2p. Fe 3d orbits as electron donors could narrow the band gap of $SrTiO_3$ [16].

3.3. Photocatalytic hydrogen evolution of samples

In the case of the Pt loading $SrTiO_3$ system, an electron must migrate to the Pt surface and a hole to the $SrTiO_3$ surface where both sites are well separated. In the case of H_2 evolution from aqueous methanol solution, holes are consumed irreversibly by reaction with methanol, and electrons are enriched in the catalyst [22]. The photocatalytic activities of $SrTiO_3$ through the PC method for hydrogen evolution are shown in Fig. 10. The rates of photocatalytic hydrogen evolution over PC500, PC600, PC700, PC800, and PC1000 are R_{PC500}, R_{PC600}, R_{PC700}, R_{PC800}, and R_{PC1000}. The order of hydrogen generation rates for $SrTiO_3$ is as follows: $R_{PC600} > R_{PC700} > R_{PC500} > R_{PC800} > R_{PC1000}$ (the rate of photocatalytic activity shown in Table 1). The result shows that photocatalytic activity of hydrogen evolution over $SrTiO_3$ is dependent on the size of $SrTiO_3$. The size order of $SrTiO_3$ is as follows: PC600 < PC700 < PC800 < PC1000. The rates of photocatalytic hydrogen evolution of PC600, PC700, PC800, and PC1000 are 3.2, 2.6, 1.8, 0.57 mmol h^{-1} g^{-1}. Although PC500 has the smallest size,

Table 1
Synthesis condition of $SrTiO_3$, crystal type, average particle size, band gap and rate of hydrogen generation

Sample name	Calcined temperature (°C)	Calcination time (h)	Crystal type	Average particle size (nm)	Band gap (eV)	Rate of hydrogen generation (mmol h^{-1} g^{-1})
PC500	500	5	Cubic	25	3.1	2.0
PC600	600	5	Cubic	30	3.1	3.2
PC700	700	5	Cubic	40	3.1	2.6
PC800	800	5	Cubic	90	3.1	1.8
PC1000	1000	5	Cubic	110	3.1	0.57
S800/3/1000/3	800/1000	3/3	Cubic	140	3.1	1.3
S800/5	800	5	Cubic	150	3.1	1.0
S800/5/1000/3	800/1000	5/3	Cubic	150	3.1	0.18
Q800/2	800	2	Cubic	30	2.0	0.0082

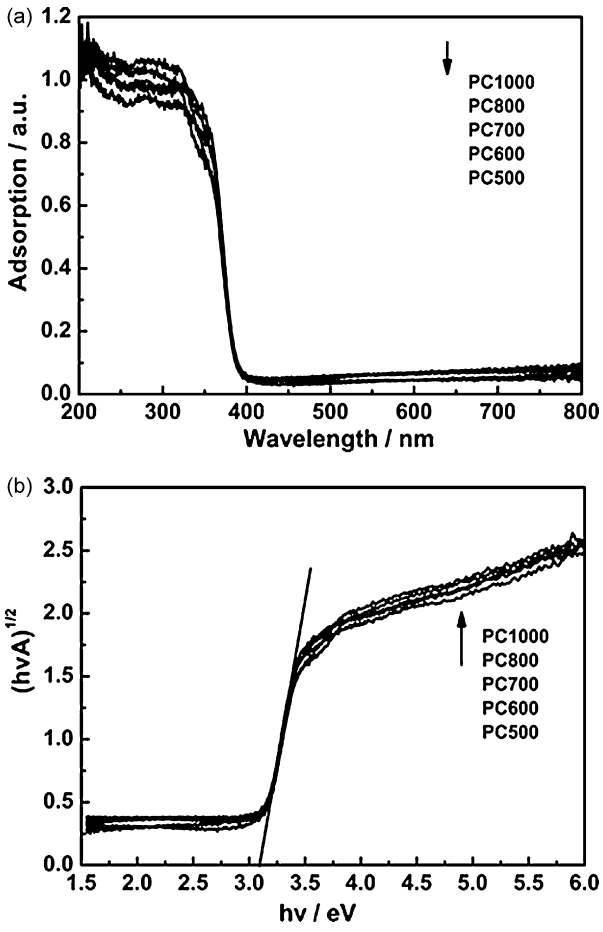

Fig. 8. UV–vis diffuse reflectance spectra of $SrTiO_3$ synthesized by PC method calcined at different temperatures. (a) Plots of adsorption vs. wavelength of light and (b) plots of square root of $h\nu(A)$ vs. $h\nu$.

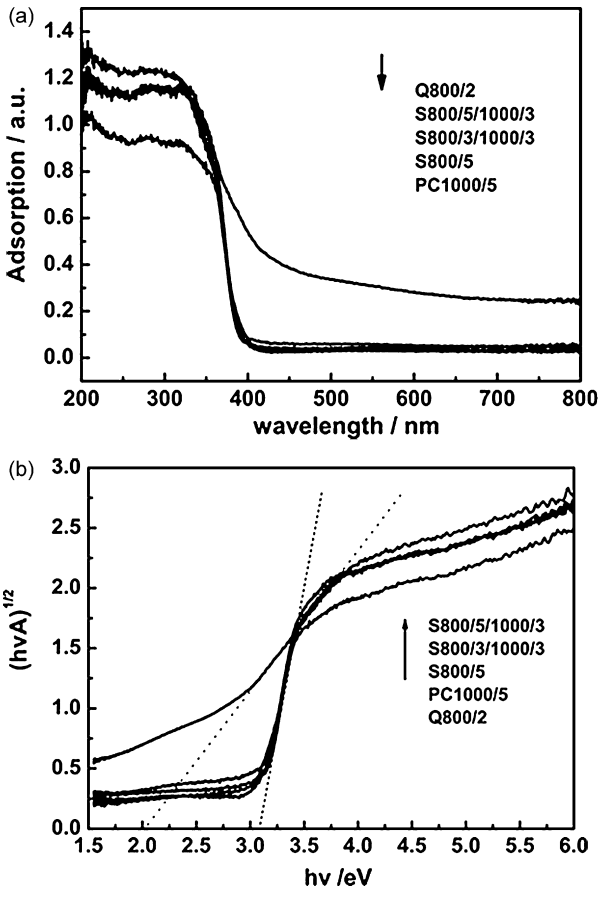

Fig. 9. UV–vis diffuse reflectance spectra of $SrTiO_3$ synthesized by solid state reaction and milling assistant methods. (a) Plots of adsorption vs. wavelength of light; (b) plots of square root of $h\nu(A)$ vs. $h\nu$.

remnant carbons exist on the surface of PC500, which block the active sites on the photocatalysts and affect negatively the photocatalytic activity of hydrogen evolution. R_{PC500} is 2.0 mmol h^{-1} g^{-1}. PC600 has the highest photocatalytic activity for hydrogen evolution, 3.2 mmol h^{-1} g^{-1}, because of its carbon-free makeup, small particle size, and large surface area. Small particles have numerous active sites exposed on their surface. These active sites may absorb more water molecules, which are reduced by photoproduction electrons. In addition, small particles could shorten the diffusion distance from the interior to the surface of the photocatalyst for photoproduction electrons and holes.

Fig. 11 demonstrates the photocatalytic activities of hydrogen evolution over $SrTiO_3$ through the solid state and milling assistant methods under UV light. The rates of photocatalytic hydrogen evolution of S800/5, S800/3/1000/3, S800/5/1000/3, and Q800/2 are denoted as $R_{S800/5}$, $R_{S800/3/1000/3}$, $R_{S800/5/1000/3}$, and $R_{Q800/2}$.

In the solid state method, $R_{S800/5}$, $R_{S800/3/1000/3}$ and $R_{S800/5/1000/3}$ are 1.0, 1.3, and 0.18 mmol h^{-1} g^{-1}. The order of photocatalytic activity of hydrogen evolution is as follows: $R_{S800/3/1000/3} > R_{S800/5} > R_{S800/5/1000/3}$. This result demonstrates that the preliminary treatment is a key factor affecting the photocatalytic activity of hydrogen evolution. S800/5, S800/3/1000/3, and S800/5/1000/3 with similar sizes have different surface status. S800/3/1000/3 samples have more active sites than S800/5 and S800/5/1000/3. S800/5/1000/3 agglomerates to some extent.

According to the rate of photocatalytic hydrogen evolution, $SrTiO_3$ from the PC method has better photocatalytic activity of hydrogen evolution than those through solid state reaction. $SrTiO_3$ from the PC method have small sizes and good uniformity of components. Small size is a favorable factor for improvement of the photocatalytic activity of hydrogen evolution because more active sites are exposed. In the PC method, reactants contact at the molecular level, which makes the components of $SrTiO_3$ uniform. Good uniformity of $SrTiO_3$ components could make excited photogenerated electrons and photogenerated holes transport easily.

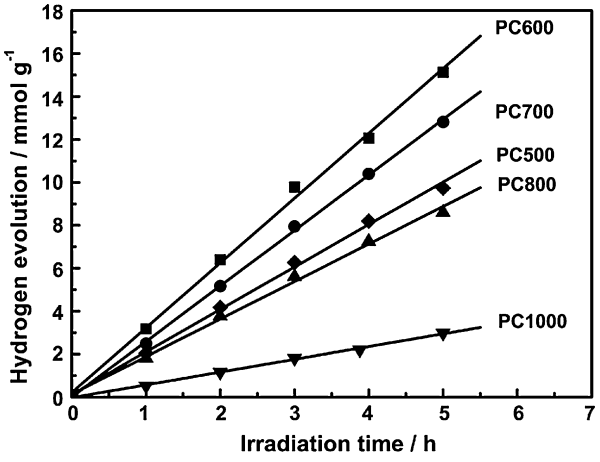

Fig. 10. Photocatalytic hydrogen evolution of $SrTiO_3$ through PC method (PC500, PC600, PC700, PC800, and PC1000).

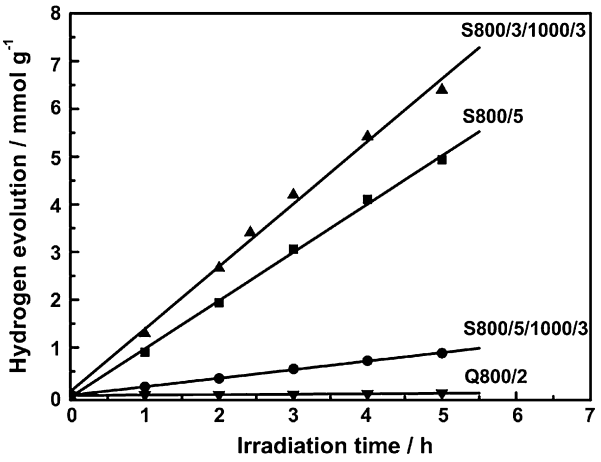

Fig. 11. Photocatalytic hydrogen evolution of $SrTiO_3$ samples through solid state and milling assistant methods (S800/5, S800/3/1000/3, S800/5/1000/3, and Q800/2).

The Q800/2 has the lowest rate of photocatalytic hydrogen evolution under UV light among $SrTiO_3$ samples. Q800/2 with bad gap of 2.1 eV could adsorb visible light. In addition, agglomeration of Q800/2 nanoparticles in some extent negatively affects the photocatalytic activities of hydrogen evolution under UV light.

4. Conclusions

The synthesis method of $SrTiO_3$ could affect the photocatalytic activity of hydrogen evolution under UV light by splitting methanol–water solutions. The surface status of $SrTiO_3$ through the three methods is different. The PC method is used to synthesize $SrTiO_3$ with small size and uniform components. The photocatalytic activity of hydrogen evolution over PC600 under UV light is the best, 3.2 mmol h^{-1} g^{-1}. $SrTiO_3$ particles from the solid state method in our work have smaller sizes than those from the classic solid state method. However, $SrTiO_3$ particles from the solid state method have relatively large sizes and sinter to a greater extent than those from PC method. The photocatalytic activity of $SrTiO_3$ from the solid state method is worse than that from the PC method. The milling assistant method could be used to synthesize cubic $SrTiO_3$ with small sizes. However, iron doping into $SrTiO_3$ and agglomeration of $SrTiO_3$ nanoparticles make its photocatalytic activity of hydrogen evolution under UV light worst among the three methods.

The PC method is potent for synthesizing $SrTiO_3$ nanoparticles and other layered perovskite-type compounds with better photocatalytic activity of hydrogen evolution under UV light. The cation-doped $SrTiO_3$ can adsorb visible light and be used to realize photocatalytic hydrogen evolution under visible light. The PC and milling assistant methods can be used to prepare perovskite compounds doped with metal ions.

Acknowledgements

The authors acknowledge support from the National Natural Science Foundation of China (Nos. 20221101 and 20671004), MOST of China (No. 2006AA05Z130), MOE of China (No. 707002), the Beijing Municipal Commission of Education (No. KM 20031141714), and the Beijing Foundation for Elitists (No. 20051D0502208).

References

[1] K. Honda, A. Fujishima, Nature 238 (1972) 37–39.
[2] M. Kazuhiko, D. Kazunari, J. Phys. Chem. C 111 (2007) 7851–7861.
[3] M. Ni, M.K.H. Leung, D.Y.C. Leung, K. Sumathy, Renew. Sust. Energ. Rev. 11 (2007) 401–425.
[4] Z.G. Zou, J.H. Ye, K. Sayama, H. Arakawa, Nature 414 (2001) 625–627.
[5] K. Domen, A. Kudo, T. Onishi, J. Catal. 102 (1986) 92–98.
[6] C.T.K. Thaminimullla, T. Takata, M. Hara, J.N. Kondo, K. Domen, J. Catal. 196 (2000) 362–365.
[7] S. Thammanoon, N. Supachai, S. Yoshikazu, Y. Susumu, J. Mol. Catal. A 235 (2005) 1–11.
[8] X.Y. Chen, T. Yu, X.X. Fan, H.T. Zhang, Z.S. Li, J.H. Ye, Z.G. Zou, Appl. Surf. Sci. 253 (2007) 8500–8506.
[9] A. Kudo, A. Tanaka, K. Domen, T. Onishi, J. Catal. 111 (1998) 296–301.
[10] J.S. Wang, S. Yin, J. Photochem. Photobiol. A 187 (2007) 72–77.
[11] B.R. Kim, T.U. Kim, W.J. Lee, J.H. Moon, B.T. Lee, H.S. Kim, J.H. Kim, Thin Solid Film 515 (2007) 6438–6441.
[12] Y. Qin, G.Y. Wang, Y. Wang, J. Catal. Commun. 8 (2007) 926–930.
[13] R. Konta, T. Ishii, H. Kato, A. Kudo, J. Phys. Chem. B 108 (2004) 8992–8995.
[14] H. Kato, A. Kudo, J. Phys. Chem. B 106 (2002) 5029–5034.
[15] D.F. Wang, J.H. Ye, T. Kako, T. Kimura, J. Phys. Chem. B 110 (2006) 15824–15830.
[16] H. Irie, Y. Maruyama, K. Hashimoto, J. Phys. Chem. C 111 (2007) 1847–1852.
[17] A. Kudo, A. Tanaka, K. Domen, T. Onishi, J. Catal. 111 (1988) 296–301.
[18] D. Wang, J. Ye, T. Kako, T. Kimura, J. Phys. Chem. B 110 (2006) 15824–15830.
[19] D. Hwang, H. Kim, J. Lee, J. Kim, W. Li, S. Oh, J. Phys. Chem. B 109 (2005) 2093–2102.
[20] H. Jeong, T. Kim, D. Kim, K. Kim, Int. J. Hydrogen Energy 31 (2006) 1142–1146.
[21] R. Abe, M. Higashi, K. Sayama, Y. Abe, H. Sugihara, J. Phys. Chem. B 110 (2006) 2219–2226.
[22] J.S. Jang, H.G. Kim, V.R. Reddy, S.W. Bae, S.M. Ji, J.S. Lee, J. Catal. 231 (2005) 213–222.